Journal of Molecular Structure 1317 (2024) 138992

Contents lists available at ScienceDirect

Journal of Molecular Structure

journal homepage: www.elsevier.com/locate/molstr

Investigation of structural, morphological and optoelectronic properties of (Ni, Co)-doped and (Ni/Co) co-doped SnO_2 (110) sprayed thin films

Warda Darenfad [a,*], Noubeil Guermat [b], Nadir Bouarissa [c], Kamel Mirouh [a]

[a] Thin Films and Interfaces Laboratory (LCMI), University of Constantine 1, 25000 Constantine, Algeria
[b] Department of Electronics, Faculty of Technology, University of M'sila, PO Box 166 Ichebilia, 28000 M'sila, Algeria
[c] Laboratory of Materials Physics and Its Applications, University of M'sila, 28000 M'sila, Algeria

ARTICLE INFO

Keywords:
Thin films
(Ni/Co) co-doped SnO_2
Hydrophibic
Hydrophilic

ABSTRACT

The manuscript details the application of spray pyrolysis for the deposition of an economically viable transparent conductive oxide film comprised of (Ni/Co) co-doped SnO_2 on a glass substrate. The primary objective of this research was to systematically examine the impact of Ni/Co co-doping on diverse properties of the SnO_2 thin film. These properties encompassed the film's structural composition, surface morphology, optical response, and electrical behaviors. A comparison was made with pure SnO_2 film, as well as SnO_2 films doped with 3 %Ni and 1 %Co. The results indicate that all the samples exhibited a tetragonal structureThe introduction of Co and Ni atoms had no impact on the favored alignment of the (110) plane or the crystal structure of the SnO_2 film. The crystallite size of the pure SnO_2 film, as well as the (Co, Ni)-doped and (Ni/Co) co-doped SnO_2 films, varied within the range of 11 to 20 nm. Scanning electron microscopy (SEM) images were employed to assess how doping and co-doping influenced the surface characteristics of the films. The presence of pores and/or roughness on the surface resulted in a hydrophilic character and a decrease in the contact angle for the doped films (Ni, Co). However, the co-doped film exhibited a hydrophobic characteristic due to the surface enhancement provided by SnO_2:3 %Ni:1 %Co. The research also focused on the optical characteristics of the films, showing a positive impact with the proper incorporation of Ni and Co atoms into the SnO_2 lattice. It was notably observed that the addition of Ni and Co atoms improves the optical properties of the undoped transparent SnO_2 film in the visible spectrum, with a high transmittance of 87 % achieved for the Ni-doped film. Furthermore, the hydrophobic nature achieved by adding a concentration of 3 %Ni to the SnO_2:1 %Co film enhances its optical transmission in the range of 300 nm to 750 nm. The SnO_2 film shows an improvement in the electrical resistivity upon doping and co-doping with low resistivity value of 2.22×10^{-2} Ω.cm for the film (3 %Ni/1 %Co)-SnO_2. Drawing from these insightful results, the study proposes the potential utilization of (Ni/Co) co-doped SnO_2 films as transparent electrodes in optoelectronic applications, especially in the manufacturing of thin film solar cells.

1. Introduction

Tin dioxide (SnO_2) is widely preferred in the field of solar cells due to its remarkable properties such as high chemical and mechanical stability and low cost [1]. However, the use of SnO_2 in the fields of optoelectronics is influenced by two essential factors: intrinsic defects and the introduction of dopants. The electrical conductivity of undoped SnO_2 is associated with the presence of oxygen vacancies, native defects and tin interstitials. Thus, the regulation of these native defects is essential to control the conductivity of the material. Generally speaking, it is possible to improve both the electrical conductivity and optical transmission of SnO_2 by promoting the formation of oxygen vacancies and introducing some impurity atoms [2]. According to several studies in the literature, doping the SnO_2 lattice with elements such as zinc (Zn) [1], nickel (Ni) [3], cobalt (Co) [4], and fluorine (F) [5] has been shown to be beneficial in improving its optoelectronic properties. Among the various studied dopants, we focus on the study of Co for several reasons: (i) Under light excitation, cobalt undergoes ionization, passing from the Co^{+2} cation to the Co^{+3} cation, thus releasing an electron which migrates towards the conduction band. This process contributes to an improvement in the electrical conductivity of films under light excitation. (ii) The ionic radius of cobalt Co^{+2} (0.058 nm, [6]) is smaller and

* Corresponding author.
E-mail address: daranfed.warda@umc.edu.dz (W. Darenfad).

https://doi.org/10.1016/j.molstruc.2024.138992
Received 21 February 2024; Received in revised form 18 May 2024; Accepted 10 June 2024
Available online 10 June 2024

more stable than that of tin Sn^{+4} (0.071 nm, [3]). (iii) The introduction of cobalt offers the possibility of regulating the optical properties of the material. (iv) Cobalt exhibits corrosion resistance, which improves the corrosion resistance of the matrix compound. Furthermore, nickel (Ni) presents significant appeal in this research due to its non-toxicity and its ease of use as a dopant. Additionally, the nickel cation (Ni^{+2}) displays an ionic radius of approximately 0.069 nm, slightly smaller than that of tin (Sn^{+4}) [2]. However, its electro-negativity is lower than that of tin, with a value of around 1.91 Pauling compared to around 1.96 Pauling for tin [2]. These characteristics suggest the possibility of incorporation of nickel cations into the SnO_2 crystal lattice. According to the literature, there are a few studies that focus on the structural, morphological, optical and electrical properties of SnO_2 films doped with nickel [3-4] or cobalt [4]. The introduction of the Ni dopant into SnO_2 was associated with an increase in the crystallite size as well as an improvement in the transmittance of the material, accompanied by a reduction in the band-gap width [3]. According to Park et al. [7], doping SnO_2 with cobalt induces an increased concentration of charge carriers, which could improve electrical conductivity. These studies therefore highlight the potential of the remarkable properties of cobalt and nickel as dopants in SnO_2. However, the observation of a lack of in-depth studies on the co-doping of these elements in the tin oxide network motivated the realization of the present study. Various physical and chemical methods have been used to produce thin films of SnO_2 doped in the form of nanostructures. Among these methods, spray pyrolysis (SP) has gained attention due to its many advantages, including its simplicity, cost-effectiveness, and ability to produce homogeneous films. Additionally, SP enables the efficient incorporation of doping elements into the SnO_2 matrix, which improves the desired physicochemical properties for a wide range of applications. Surface wettability is an important aspect of surface properties and has significant implications for photovoltaic applications [8-9]. Surfaces can be classified according to the contact angle (CA, θ) as hydrophilic ($\theta < 90°$) or hydrophobic ($\theta > 90°$) [8-10]. Hydrophobic surfaces, in particular, have shown promise for clear coats. This characteristic ensures optimal sunlight transmission through the solar cell, enhancing the efficient conversion of solar energy into electricity. For instance, Guermat et al. [5] conducted a study focusing on the synthesis and characterization of wettability, along with various physical properties, of tin oxide (SnO_2) doped with varying concentrations of fluorine (0 %, 8 %, 10 % and 12 %) deposited via spray pyrolysis. They confirmed that the hydrophobic nature enhances the physical properties of the SnO_2:12 %F film, rendering it more suitable for use as a transparent conductive layer in solar cells. Furthermore, Darenfed et al. [11] observed that the hydrophobic nature improves the optical and electrical properties of zinc oxide film doped with 1 %Mg and co-doped with 1 %Mg:6 %F deposited via spray pyrolysis. These intriguing findings have sparked our interest in the significance of this hydrophobic characteristic for transparent films in thin-film solar cells.

In this study, the primary objective is to develop hydrophobic thin film of SnO_2 co-doped with Co and Ni, elaborated via spray pyrolysis on ordinary glass substrate. To the author's knowledge, this area has only been explored in a handful of published works. In light of this, an effort is made to synthesize pure SnO_2 films as well as SnO_2 films doped with 3 %Ni, 1 %Co, and a combination of 3 %Ni and 1 %Co, and to investigate the effect of Co and Ni levels on structural, morphological, wettability, optical, and electrical properties. To our knowledge, this is the first study to explore the wettability of spray-deposited thin films of SnO_2:3 %Ni:1 %Co, highlighting the novelty of our work.

2. Experimental

In our study, the sprayed solution for depositing the thin films was prepared using $SnCl_2{\cdot}2H_2O$ (tin chloride dihydrate) as the tin precursor and $NiCl_26H_2O$ (nickel chloride hexahydrate) and $CoCl_2H_2O$ (cobalt chloride hexahydrate) as the transition metal (TM) dopants. These chemicals were obtained from Sigma-Aldrich with high purity levels. The fixed mass ratio of 3 % for nickel and 1 % for cobalt in this work, in order to study the individual and combined effects of these dopants on the properties of SnO_2 films. A mixture of $SnCl_2{\cdot}2H_2O$ and the corresponding metal chloride salts was prepared to form the solution for deposition. The different films are produced for a temperature of 400 °C, a duration of 7 min and a nozzle-substrate distance = 17 cm. To characterize the structural properties of the deposited films, X-ray diffraction (XRD) analysis was conducted utilizing a Philips X'Pert system equipped with CuKα radiation (wavelength $\lambda CuK\alpha = 1.5418$ Å). The surface morphology and microstructure were investigated by scanning electron microscope (SEM) embedded with an Energy Dispersive x-ray (EDS) system (FEI Quanta 450 FEG). The contact angle of each deposit was measured by placing a 5 µl drop of distilled water on the film surface and recording the contact angle after 5 s. For the determination of film thickness, we employed a DECTAK3 type profilometer. To assess the optical transmission characteristics within the UV–Visible range (300–800 nm), we conducted measurements using a Shimadzu UV-3101 PC spectrophotometer. For a comprehensive understanding of the electrical properties, specifically resistivity, the thin films underwent characterization through the four-probe method, utilizing a Keithley 2401 instrument, all performed at room temperature. These experimental approaches provided a thorough analysis of the physical and optical features, as well as the electrical performance of the thin films under investigation.

3. Results and discussion

In Fig. 1, the XRD spectra of the SnO_2 films show diffraction peaks in the 2θ range from 20° to 110° The most prominent peak observed at $2\theta = 26.37°$ corresponds to the (110) plane of tetragonal SnO_2. Additional less intense peaks can be attributed to other crystallographic directions such as (101), (200), (211), (220), (310), (301) and (321). The X-ray diffraction (XRD) peaks observed in all the fabricated films align well with the JCPDS database (sheet n° 41–1445) [1,3], confirming the tetragonal structure with a rutile phase of the SnO_2 nanostructures in pure, doped, and co-doped films. This indicates that the addition of Ni and Co dopants does not introduce any secondary phases into the SnO_2 films. The experimental findings further elucidate that the intensity of the most prominent peak, specifically the (110) peak, is influenced by the doping and co-doping concentrations. The intensity and refinement of the (110) peak increase for the SnO_2:3 %Ni and SnO_2:1 %Co, suggesting an enhancement in the crystalline quality of the films. This improvement in diffraction intensity is attributed to the systematic arrangement of atoms on the crystal surface and grain interfaces [12, 13]. Conversely, in the case of co-doping, there is a notable decrease in intensity coupled with an observable widening at mid-height of the (110) peak. This decrease could be attributed to the non-ideal incorporation of dopants into the matrix, which disrupts the crystal growth in the (110) direction, indicating a degradation in crystalline quality. Another possibility is that double doping induces additional defects or stresses that affect X-ray diffraction, leading to a decrease in the intensity of this peak. The outcomes observed align cohesively with established literature, notably exemplified by the research conducted by Guermat et al. [1], which delved into the impact of Zn doping on SnO_2 films deposited through spray pyrolysis Fig. 1.

Fig. 2 presents a zoom of XRD spectra at (110) diffraction peak region for 2θ close to 24.5° - 30° As observed, when Ni or Co are incorporated into the SnO_2 matrix, there is a shift of the (110) peak to higher angles. This shift is attributed to an increase in the intensity of the (110) peak and an enhancement in the orientation of the crystallites. This indicates that the doping of Ni or Co has a distinct effect on the crystalline structure of the film, a finding that aligns with similar observations in existing literature [4,14]. Conversely, for Ni/Co co-doping, a shift of the (110) peak towards smaller angles compared to doped films is observed. The same result was observed by Zulfiqar et al. [15] and Divya et al. [16]. This shift can be explained by the substitution of Ni and Co for tin

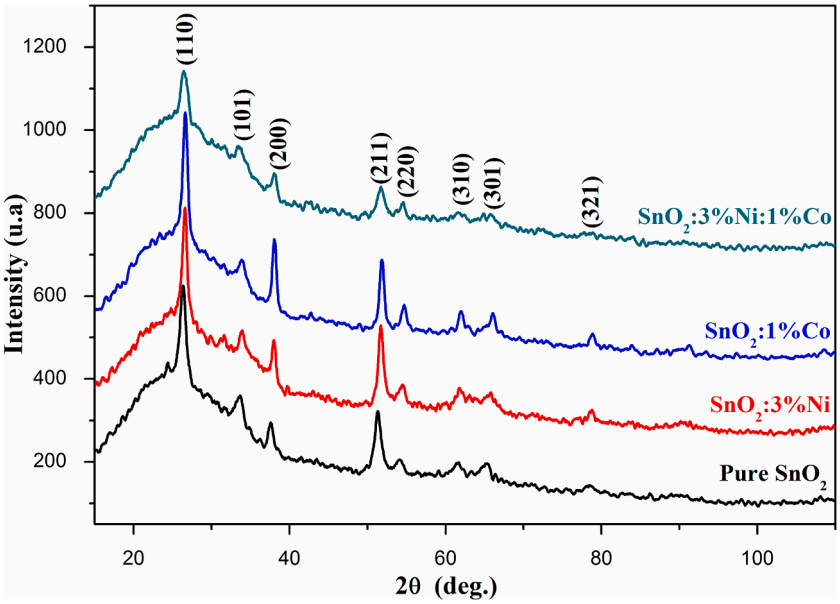

Fig. 1. XRD pattern of pure, Ni- and Co-doped and (Ni, Co) co-doped SnO_2 nanostructures.

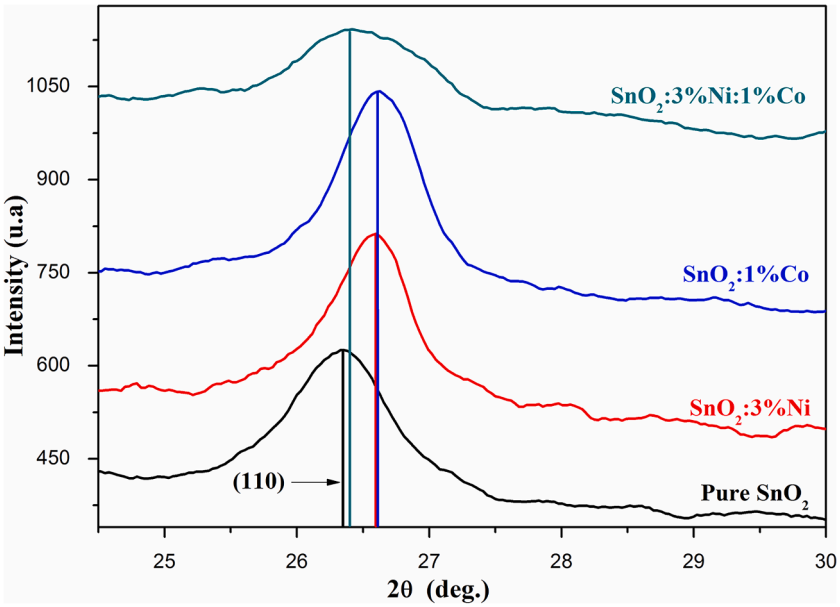

Fig. 2. Zoom of (110) Peak positions and intensities of X-ray diffraction of obtained films.

(Sn) atoms in the SnO_2 structure, which alters the inter-atomic distances in the crystal structure. Furthermore, a higher density of dopants can modify the crystal structure of SnO_2, leading to the (110) peak shifting to smaller angles.

The Debye-Scherrer formula serves as a valuable tool for estimating the crystallite size (D) of nanocrystalline materials based on X-ray diffraction (XRD) data. This formula is mathematically expressed as follows [17-18]:

$$D = \frac{0.9\lambda}{\beta\cos\theta} \tag{1}$$

In this formula, λ represents the wavelength of the X-ray, β corresponds to the full width at half maximum (FWHM) of the diffraction peak, θ denotes the angle of diffraction, and (hkl) signifies the specific set of diffracted crystallographic planes.

The relationship frequently employed for the estimation of dislocation density (δ) is articulated as follows:

$$\delta = \frac{1}{D^2} \tag{2}$$

The strain values (ε) of the films were calculated using the following formula:

$$\varepsilon = \frac{\beta\cos\theta}{4} \tag{3}$$

The values of D, FWHM, δ and ε of the samples are grouped in Table 1.

From Table 1, it is evident that there is an increase in the crystallite size of Ni- and Co-doped SnO_2 films, measuring 19 nm and 20 nm, respectively, compared to the undoped SnO_2 films, which had a size of 13 nm. This observed increase in crystallite size can be attributed to the enhancement in structural integrity introduced by the doping process in

Table 1
The structural parameters derived for the pure, (Ni, Co)-doped and (Ni/Co) co-doped SnO_2 samples.

Sample type	Thickness, (nm)	D, nm	δ, $(nm)^{-2}$	ε, $(\times 10^{-3})$
Pure SnO_2	324	13	0.00554	2.580
SnO_2:3 %Ni	280	19	0.00291	1.871
SnO_2:1 %Co	300	20	0.00254	1.747
SnO_2:3 %Ni:1 %Co	420	11	0.00878	3.248

the films, as well as the reduction in dislocation density, as depicted in Table 1. This behavior is consistent with findings in the literature [4] for SnO_2 films doped with Ni and Co in concentrations ranging from 0 % to 4 % using the spray pyrolysis method. Soussi et al. [4] suggest that the increase in crystallite size (D) may be correlated with a decrease in the prevalence of defects, particularly grain boundaries and dislocation density, within the films. Toloman et al. [19] also suggested that the increase in D is associated with a decrease in oxygen content in the SnO_2 network caused by doping, leading to a reorganization of the SnO_2 structure. On the flip side, there is a noticeable reduction in the crystallite size within the co-doped film. This decrease in crystallite size can be interpreted by several factors. First, the simultaneous incorporation of Ni and Co into the SnO_2 matrix can disrupt crystallite growth, leading to a smaller size. Furthermore, the replacement of some Sn atoms with Ni and Co in the SnO_2 crystal structure can modify the inter-atomic interactions and growth dynamics of crystallites, thus influencing their final size. Finally, the presence of these dopants can also increase the strain and dislocation density (see Table 1), which can limit crystallite growth and contribute to a smaller size. Similar observations were made by Dakhel [20] in SnO_2:3 %Ni:5 %Ga and SnO_2:3 %Ni:5 %Zn films deposited via the co-precipitation method. The decrease in D in co-doped films suggests that the dopant ions partially accumulate at the crystallite boundaries, hindering their growth. Additionally, the reduction in D can be attributed to the shrinkage of the unit cell volume resulting from the substitution of Sn^{+4} with Co^{+2} and Ni^{+2}.

The examination of morphological features in thin films, including pure, (Co, Ni)-doped and (Ni/Co) co-doped SnO_2, was conducted through scanning electron microscopy (SEM), as depicted in Fig. 3. The images clearly depict significant alterations in the morphology of the deposited films, which are direct consequences of the doping and co-doping processes. In the pure SnO_2 film, the grains exhibit non-uniform "nanoflower"-like shapes, with varied sizes and uneven distribution on the surface. This heterogeneity in grain shape and size leads to irregular distribution across the film. However, the SEM image of Ni-doped SnO_2 film (Fig. 3(b)), it shows nanotubes that appear to be organized and homogeneously distributed, for Fig. 3(c), shows that the layer is rough with the existence of a certain number of pores making them more suitable for the gas sensor application. The nanostructures of the co-doped SnO_2 film undergo a notable morphological transformation, manifested by an aggregation of regular and well-defined lamellar grains, as observed in the high-resolution SEM images (Fig. 3 (d)). This change can be attributed to the increase in film thickness (Table 1), which can have a significant impact on grain growth and their mutual interaction during the development phase, while decreasing the presence of surface defects, notably pores of the matrix. This increase in thickness could promote the formation of more regular and better organized lamellar grains, potentially contributing to surface densification. From this analysis, it can be concluded that the co-doped SnO_2 film exhibits a smooth and uniform surface, a characteristic that holds significant promise for its utility as an optical window in solar cell applications.

The EDS-spectrum analysis was employed to discern the compositional presence of chemicals in the prepared samples, as illustrated in Fig. 4. The EDS spectrum distinctly indicates that in the pure SnO_2 sample, Sn and O are the predominant elemental species. In contrast, the (Co, Ni)-doped SnO_2 sample exhibits additional peaks corresponding to Co and Ni. The presence of a Si peak can be attributed to the Si substrate. According to the data presented in this figure, a substantial decrease in the Sn concentration is evident in the Ni-doped sample, contrasted by a notable increase in the Si peak compared to the remaining samples. This

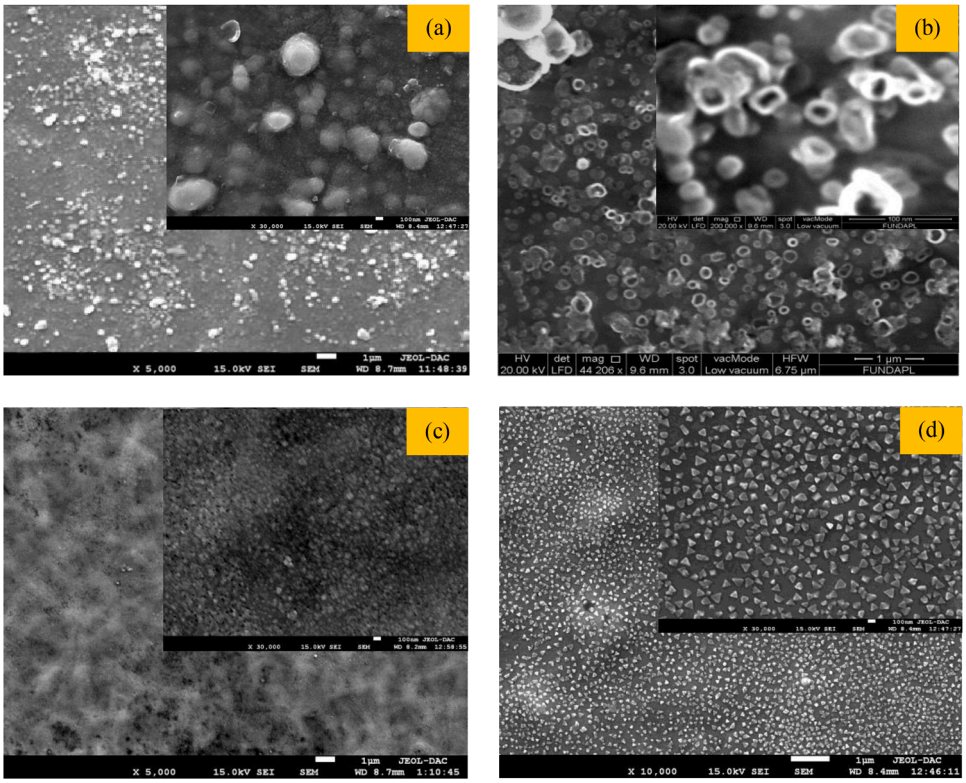

Fig. 3. SEM of (a) pure, (b) SnO_2:3 %Ni, (c) SnO_2:1 %Co and SnO_2:3 %Ni:1 %Co nanostructures.

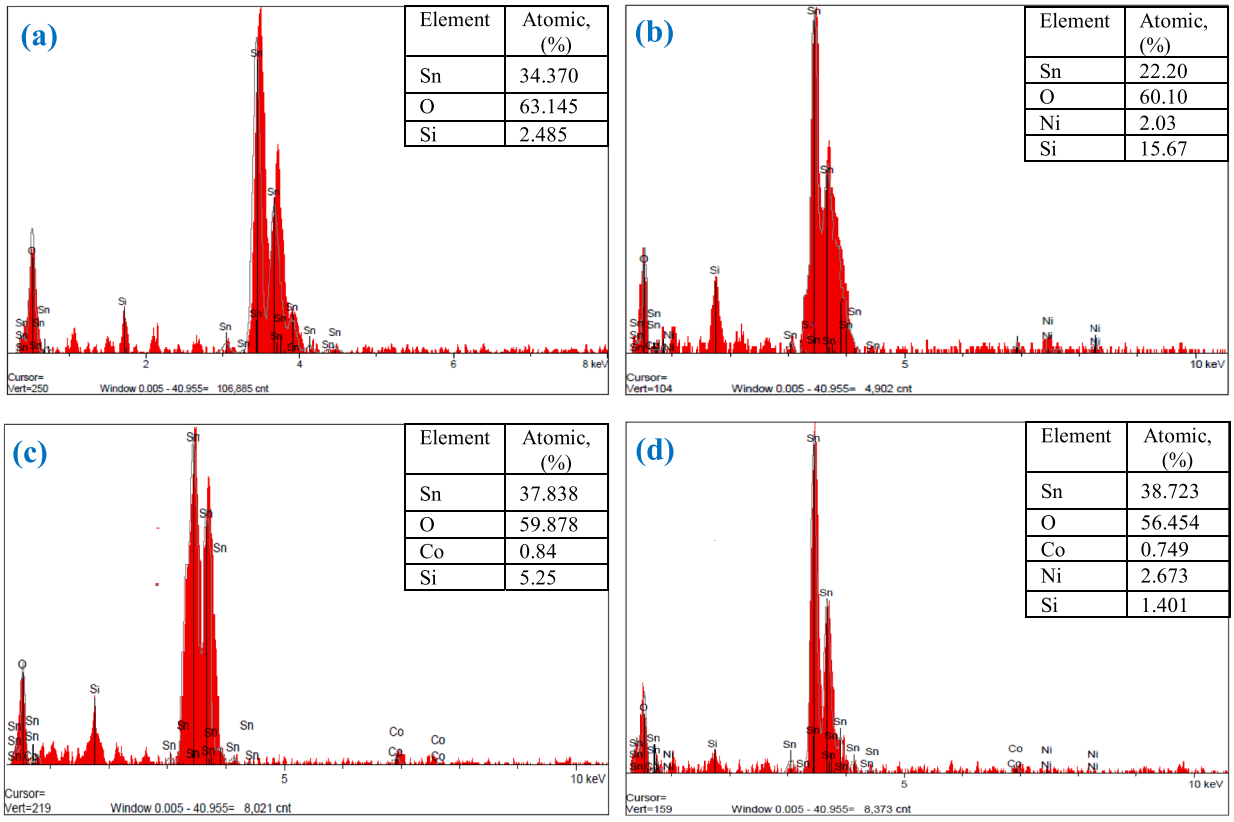

Fig. 4. EDS spectrum of (a) pure, (b) 3%Ni-doped, (c) 1 %Co-doped and (d) 3 % Ni/1 % Co co-doped SnO_2 thin films.

trend appears to be attributable to the phenomenon of inter-diffusion. As the thickness of the SnO2:3 %Ni film decreases (down to 280 nm), the significance of interfaces between distinct layers amplifies. Consequently, inter-diffusion between the constituent elements of this layer becomes increasingly plausible. Such inter-diffusion could precipitate an increase in the prevalence of silicon in the deeper layers of the sample (SnO_2:3 %Ni), thus explaining the observed augmentation of the Si peak.

In Fig. 5, images depict water droplets with a volume of 5 µl on the surfaces of the prepared films. The average contact angle (CA, θ) was determined by measuring the drops deposited in several locations on each surface of the produced film. To mitigate the influence of evaporation, the measurements were conducted 5 s after the deposition of the water droplet.

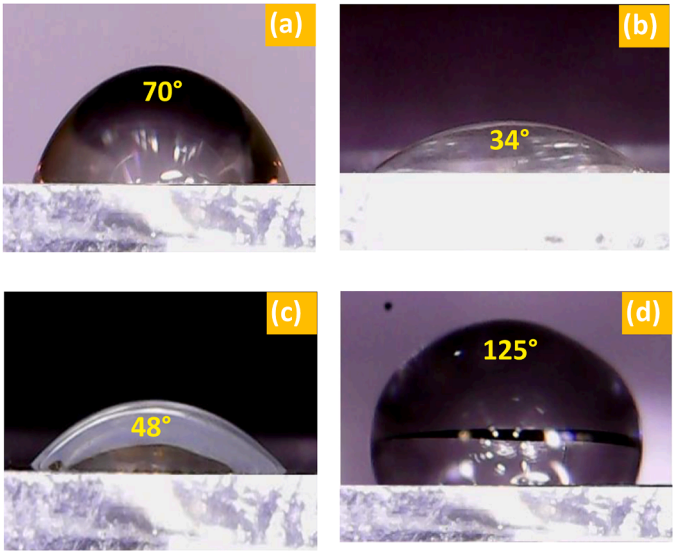

Fig. 5. Water contact angles of pure, (Ni, Co) doped and (Ni/Co) co-doped SnO_2 samples.

The contact angle values of the samples are listed in Table 2. There are some specific trends of contact angle (θ) variation for the SnO_2 films without and with doping and co-doping. Un-doped SnO_2 sample show a contact angle value of 70°, whereas for 3 %Ni-doped, 1 %Co-doped and 3 %Ni:1 %Co samples an 34°, 48° and 125° respectively was measured. Based on these results, the addition of 3 %Ni dopant to the SnO_2 film causes a decrease in the contact angle to 34°, indicating a higher hydrophilic nature compared to the pure SnO_2 sample. Similarly, the addition of 1 %Co dopant to the SnO_2 film leads to a contact angle of 48°, indicating a hydrophilic nature. The co-doped SnO_2 sample with 3 %Ni and 1 %Co shows a higher contact angle of 125°, indicating a more hydrophobic nature compared to the pure SnO_2 and singly doped samples. The transition point between hydrophilic and hydrophobic behavior is typically considered to be at a contact angle of 90° [11,21]. In this case, the doped samples (Ni-doped and Co-doped) fall into the hydrophilic range ($\theta < 90°$), while the co-doped sample falls into the hydrophobic range ($\theta > 90°$). The fluctuation in the contact angle, influenced by the effects of doping and co-doping, can be attributed to a multitude of factors. These factors encompass the size and distribution of available pores, as well as the radius of these pores [22-23], and the surface roughness [5]. This means that the surface (pores and/or

Table 2
Structural parameters obtained for pure, (Ni, Co) doped and (Ni/Co) co-doped SnO_2 samples.

Samples	Contact angle, °
Un-doped SnO_2	70
SnO_2:3 %Ni	34
SnO_2:1 %Co	48
SnO_2:3 %Ni:1 %Co	125

roughness) of the samples is changed when adding Cobalt and Nickel in different amounts with the tin oxide. Many results have shown that the addition of dopants such as Zn [1], Ni [3], F [5] and Co [24] has been previously shown to affect the surface morphology and create pores and/or roughness in the films, leading to a reduction in the contact angle. According to Khalfallah et al. [3], the presence of a porous surface generally enhances wetting and optical transmittance. Furthermore, as posited by Guermat et al. [5], the existence of surface roughness in the film is identified as a contributing factor to the reduction in both contact angle and transmittance.

The optical properties, such as transmission and optical band-gap, of undoped SnO_2 thin films, as well as those doped with Ni and Co, and co-doped with nickel and cobalt, are calculated based on the evolution of optical transmission with wavelength (λ) in the range of 300 to 800 nm. Fig. 6 depicts the transmission spectra of our spray-deposited layers on ordinary glass substrates. As observed, there is an enhancement in transmittance (T(%)) with the addition of Ni and Co dopants in the SnO_2 film compared to undoped SnO_2, with particularly high values for the SnO_2 film doped with 3 %Ni. This enhancement may stem from the good crystalline quality of these films as indicated by X-ray diffraction results. It's noteworthy that the transmission improvement of Ni and Co-doped films achieved in this work surpasses that reported by Soussi et al. [4] for the same dopants deposited via spray pyrolysis. However, the addition of 3 %Ni to the SnO_2:1 %Co film increases the optical transmission of the SnO_2:1 %Co film in the range of 300 nm to 750 nm. This increase could be attributed to the higher concentration of Ni compared to Co, on one hand. On the other hand, this behavior is likely due to the hydrophobic nature of the co-doped film, as indicated by the contact angle analysis. This behavior is comparable to the study of the optoelectronic characteristic of thin films of Ni-doped SnO_2 and co-doped with Ni and Al prepared by the spray pyrolysis technique [2].

Fig. 7 shows Tauc's plots of our films. The energy value of the forbidden band (Eg) of the produced films can be approximated using the Tauc equation. This equation delineates the correlation between the optical absorption coefficient (α) and the energy of incident photons (hυ), as expressed below [17]:

$$\alpha h\nu = const..\left(h\nu - E_g\right)^{1/2} \quad (4)$$

Where, const. is a constant independent of energy. The linear part of the Tauc's plots provides the values of Eg for different films, which are calculated as 3.32, 4, 3.41 and 3.7 eV for pure, 3 %Ni, and 1 %Co, 3 % Ni:1 %Co co-doped SnO_2 thin films respectively. It is observed that the gap energies of the doped and co-doped films are higher than that of pure SnO_2 (3.32 eV), with the SnO_2:3 %Ni film having the highest value (4 eV). The observed escalation in the optical bandgap with increasing dopant concentration is a phenomenon documented in various other references [25-26]. Shalan et al. [26] elaborated thin films of Zn and Ni-doped SnO_2, associating the rise in the energy bandgap with the existence of interstitially embedded (Ni and Zn) ions within the SnO_2 nanomaterials. This phenomenon can also be explained through the Burstein-Moss effect, characterized by a shift towards higher energies or a blue shift. However, for the co-doped film, a decrease and an increase in the optical gap are observed compared to the Ni and Co doped SnO_2 respectively. This decrease in the forbidden band with co-doping is attributed to the BGN effect (Band Gap Narrowing Effect) effect caused by the doping impurity cobalt. Additionally, the lower optical gap of cobalt oxide (1.5 - 2 eV, [27]) contributes to this decrease. These findings are consistent with the results published by other authors [19,28] for co-doped SnO_2 films. Furthermore, the increase in the optical gap when 3 % Ni is added to the Co doped SnO_2 film may be attributed to the larger amount of nickel (3 %) compared to cobalt (1 %). The difference in mass between these two dopants could be a contributing factor to the observed increase in the optical gap.

To ascertain the conductivity type of the deposited films, the hot probe method, specifically leveraging the Seebeck effect, was employed. The negative sign observed in the measurements serves as confirmation of the n-type conductivity exhibited by the deposited samples. Additionally, the electrical properties of the films underwent evaluation through the implementation of the four-probe measurement technique. The resistivity values obtained for various films, encompassing undoped SnO_2, cobalt-doped SnO_2, nickel-doped SnO_2, and nickel/cobalt co-doped SnO_2, are regrouped in Table 3.

According to the previous table, the variation in electrical properties shows a bell shape, increase for 3 %Ni-doped SnO_2 thin film, and then a decrease for 1 %Co-doped and (3 %Ni/1 %Co) co-doped SnO_2 thin films. The increase in resistivity with Ni can be attributed to several reasons: (i) The first reason lies in the substitution of Ni^{+2} instead of Sn^{+4} in the crystal sites, which reduces the Sn content by replacing some sites in the crystal structure [25]. (ii) The influence on the microstructure of the film, as shown in Fig. 3(b). (iii) A third reason is the formation of impurities, such as silicon (Fig. 4(b)). Similar behavior has been observed by Abdi et al. [25] in their investigation of Ni-doped SnO_2 films,

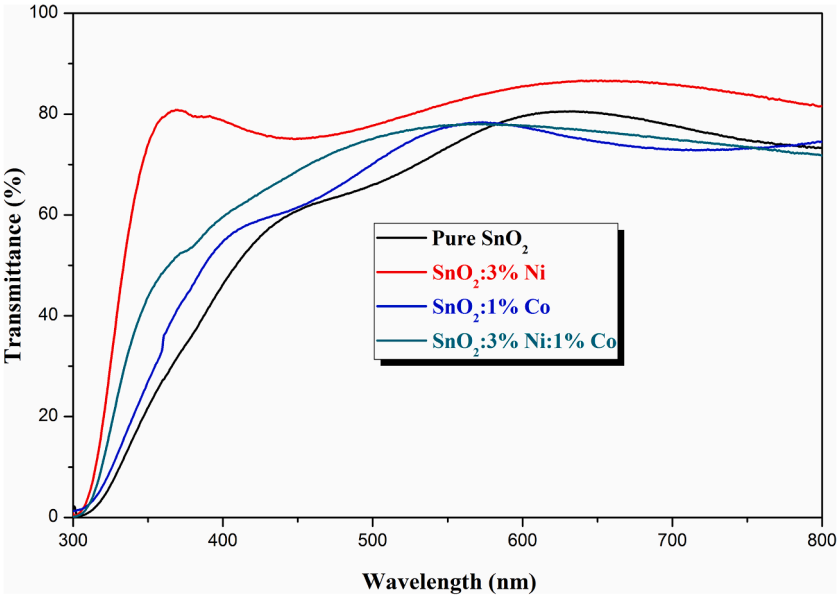

Fig. 6. UV–visible spectra of pure, (Ni, Co)-doped and (Ni/Co) co-doped SnO_2 samples.

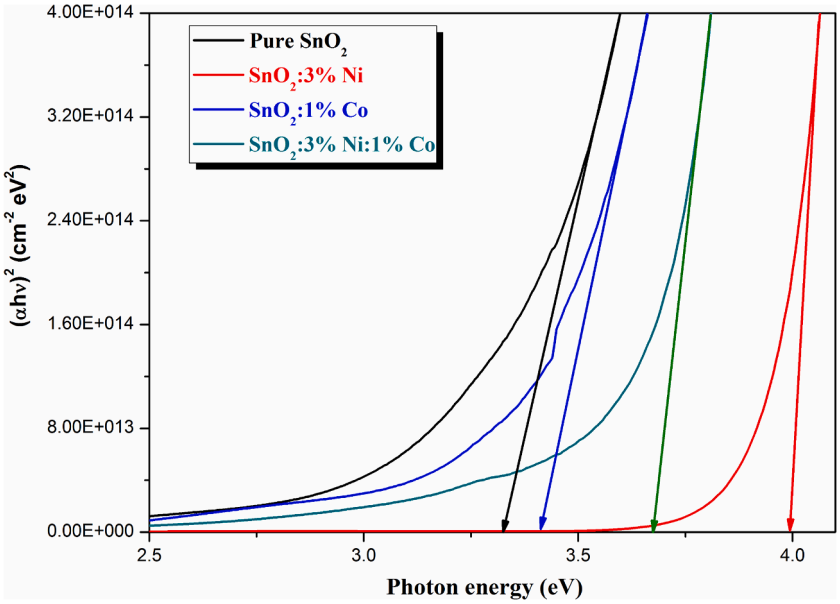

Fig. 7. Plot of $(\alpha h\nu)^2$ vs. phonon energy for pure, (Co, Ni)-doped and (Co/Ni) co-doped SnO_2 thin films.

Table 3
Variation of the resistivity of undoped, (Co, Ni)-doped and (Ni/Co) co-doped SnO_2 films for different percentages.

Sample type	Resistivity, (Ω.cm)
Undoped SnO_2	3.74
SnO_2:3 %Ni	28.57
SnO_2:1 %Co	9.4×10^{-1}
SnO_2:3 %Ni:1 %Co	2.22×10^{-2}

deposited through the sol-gel method, with Ni concentrations ranging from 0 wt.% to 20 wt.%. We note that the electrical resistivity of undoped SnO_2 (3.74 Ω.cm) is reduced with cobalt doping and takes a value equal to 9.4×10^{-1} Ω.cm which is better than that reported in the literature ($\rho = 1.14 \times 10^2$ Ω.cm) [7]. The evolution of the decrease in resistivity for SnO_2 doped with 1 % Co can be interpreted as an improvement in the electrical conductivity of the doped material. The incorporation of cobalt ions into the SnO_2 matrix can have several beneficial effects on electrical conductivity. Indeed, the smaller ionic radius of cobalt compared to that of tin allows cobalt to more easily substitute for tin atoms in the SnO_2 structure without significantly disrupting the crystal lattice. This more efficient substitution promotes better incorporation of cobalt ions into the SnO_2 structure, which contributes to greater electrical conductivity. Additionally, the presence of cobalt can help reduce defects (Table 1) and impurities in the crystal structure of SnO_2, thereby limiting the diffusion of charge carriers and improving electron mobility. The addition of 3 %Ni to the SnO_2:1 %Co film also caused a significant decrease in resistivity, with a measured value of 2.22×10^{-2} Ω.cm. This decrease in resistivity is attributed to a dual substitution process within the SnO_2 structure, where Co and Ni ions replace Sn atoms. Moreover, cobalt and nickel can act as acceptor dopants, introducing holes in the band-gap of SnO_2. This facilitates electrical conduction, further contributing to the decrease in resistivity. Furthermore, the integration of Ni and Co alters the structure of the SnO_2 film, resulting in a denser and hydrophobic surface. This surface modification plays a crucial role in reducing resistivity by enhancing the mobility of charge carriers and preventing moisture from interfering with the material's electrical properties. Similar trends of decreased electrical resistivity have been observed by Guermat et al. [6] in Ni/Co co-doped ZnO films, Ramarajan et al. [29] in Ba/Sb co-doped SnO_2 films, and by Bouabdalli et al. [2] in F/Ni co-doped SnO_2 thin films synthesized via chemical spray pyrolysis. The minimum resistivity value obtained (2.22×10^{-2} Ω.cm) is significantly lower than the $\rho = 1.02 \times 10^2$ Ω.cm that was found for the F/Ni co-doped SnO_2 deposited by spray pyrolysis [2]. It's noteworthy that this resistivity value is considered acceptable when compared to other co-doped films produced using the same technique. This implies that the chosen production method, specifically spray pyrolysis, enables the creation of co-doped films with a competitive and satisfactory resistivity for specific applications.

4. Conclusion

Undoped SnO_2, SnO_2:3 %Ni, SnO_2:1 %Co and SnO_2:3 %Ni:1 %Co thin films were successfully deposited on glass substrates using a spray pyrolysis technique. The effect of adding (Ni and/or Co) on the structural, morphological, wettability, optical, and electrical properties of SnO_2 thin films was investigated. The X-ray diffraction (XRD) analysis demonstrated that all the thin layers produced were well-crystallized, displaying a polycrystalline tetragonal structure. Furthermore, the XRD studies revealed that the preferred orientation of the films was aligned with the (110) plane, consistent with the orientation observed in the undoped layer. The images clearly illustrate significant morphological changes in the deposited films, which are directly attributed to the processes of doping and co-doping. Moreover, there is an enhancement in the surface morphology with co-doping. XRD and EDS data confirmed the good dispersion of Ni and Co atoms within SnO_2 lattice. The contact angle measurements for the undoped, SnO_2:3 %Ni, and SnO_2:1 %Co samples all registered below 90°, indicating their hydrophilic nature. However, the film SnO_2 co-doped with 3 %Ni and 1 %Co exhibited hydrophobic behavior, as evidenced by a contact angle exceeding 90° (CA = 125°). The transmittance of the films increases as Ni and Co dopants are added to the SnO_2 film, compared to pure SnO_2. Furthermore, the hydrophobic nature of the co-doped film with the addition of 3 %Ni to the SnO_2:1 %Co composition enhances its optical transmission in the 300 nm to 750 nm range. Doping and co-doping lead to an increase in the band gap of SnO_2 compared to the pure SnO_2 film. Electrical measurements performed on the co-doped film produced revealed a minimum electrical resistivity of approximately 2.22×10^{-2} Ω.cm. In conclusion, this study has clearly demonstrated that the dopants 3 %Ni and/or 1 %Co influence the physical properties of SnO_2 films. These properties show that the SnO_2:3 %Ni:1 %Co film, with its hydrophobic nature, constitutes an excellent transparent conductive

electrode for thin-film solar cells.

CRediT authorship contribution statement

Warda Darenfad: Writing – original draft, Project administration, Methodology, Investigation, Formal analysis, Data curation, Conceptualization. **Noubeil Guermat:** Writing – original draft, Visualization, Supervision, Resources, Project administration, Methodology, Investigation, Funding acquisition, Formal analysis. **Nadir Bouarissa:** Visualization, Validation, Supervision, Software, Resources, Project administration, Methodology, Investigation, Formal analysis. **Kamel Mirouh:** Writing – review & editing, Visualization, Validation, Project administration, Investigation, Data curation.

Declaration of competing interest

The authors declare that they have no known competing financial interests or personal relationships that could have appeared to influence the work reported in this paper.

Data availability

No data was used for the research described in the article.

Acknowledgements

The authors acknowledge the support from the Directorate-General for Scientific Research and Technological Development (DGRSDT-Algeria). This work has been carried out within the framework of PRFU projects N A10N01UN280120220009 and N A10N01UN190120220004 (MESRS-Algeria).

References

[1] N. Guermat, W. Darenfad, K. Mirouh, N. Bouarissa, M. Khalfallah, A. Herbadji, Effects of zinc doping on structural, morphological, optical and electrical properties of SnO_2 thin films, Eur. Phys. J. Appl. Phys. 97 (2022) 14, https://doi.org/10.1051/epjap/2022210218.

[2] E.M. Bouabdalli, M. El Jouad, T. Garmim, A. Louardi, B. Hartiti, M. Monkade, S. Touhtouh, A. Hajjaji, Elaboration and characterization of Ni and Al co-doped SnO_2 thin films prepared by spray pyrolysis technique for photovoltaic applications, Mater. Sci. Eng. B 286 (2022) 116044, https://doi.org/10.1016/j.mseb.2022.116044.

[3] M. Khalfallah, N. Guermat, W. Daranfed, N. Bouarissa, H. Bakhti, Hydrophilic nickel doped porous SnO_2 thin films prepared by spray pyrolysis, Phys. Scr. 95 (2020) 095805, https://doi.org/10.1088/1402-4896/aba8c5.

[4] L. Soussi, T. Garmim, O. Karzazi, A. Rmili, A. El Bachiri, A. Louardi, H. Erguig, Effect of (Co, Fe, Ni) doping on structural, optical and electrical properties of sprayed SnO_2 thin film, Surf. Interfaces 19 (2020) 100467, https://doi.org/10.1016/j.surfin.2020.100467.

[5] N. Guermat, W. Darenfad, K. Mirouh, M. Kalfallah, M. Ghoumazi, Super-hydrophobic F-doped SnO_2 (FTO) Nanoflowers Deposited by Spray Pyrolysis Process for Solar Cell Applications, J. Nano Electron. Phys. 15 (2022) 05013, https://doi.org/10.21272/jnep.14(5).05013.

[6] N. Guermat, W. Daranfed, I. Bouchama, N. Bouarissa, Investigation of structural, morphological, optical and electrical properties of Co/Ni co-doped ZnO thin films, J. Mol. Struct. 1225 (2021) 129134, https://doi.org/10.1016/j.molstruc.2020.129134.

[7] J.S. Park, S.S. Lee, I.K. Park, Visible and IR transparent Co-doped SnO_2 thin films with efficient electromagnetic shielding performance, J. Alloys. Compd. 815 (2020) 152480, https://doi.org/10.1016/j.jallcom.2019.152480.

[8] W. Darenfad, N. Guermat, K. Mirouh, Effect of Co-doping on Structural, Morphological, Optical and Electrical Properties of p-type CuO Films, J. Nano Electron. Phys. 15 (2023) 06009, https://doi.org/10.21272/jnep.15(6).06009.

[9] Y. Nezzari, W. Darenfad, K. Mirouh, N. Guermat, N. Bouarissa, R. Merah, Hydrophobic nickel doped Co_3O_4 sprayed thin films as solar absorber, Opt. Quant. Electron 56 (2024) 951, https://doi.org/10.1007/s11082-024-06930-6.

[10] Z. Belamri, W. Darenfad, N. Guermat, Molarity dependence of solution on structural and hydrophobic properties of ZnO nanostructures, Eur. Phys. J. Appl. Phys. 99 (10) (2024), https://doi.org/10.1051/epjap/2024230146.

[11] W. Darenfad, N. Guermat, K. Mirouh, A comparative study on the optoelectronic performance of undoped, Mg-doped and F/Mg co-doped ZnO nanocrystalline thin films for solar cell applications, J. Nano Electron. Phys. 13 (2021) 06016, https://doi.org/10.21272/jnep.13(6).06016.

[12] S.N. Matussin, A.L. Tan, M.H. Harunsani, A. Mohammad, M.H. Cho, M.M. Khan, Effect of Ni-doping on properties of the SnO_2 synthesized using Tradescantia spathacea for photoantioxidant studies, Mater. Chem. Phys. 252 (2020) 123293, https://doi.org/10.1016/j.matchemphys.2020.123293.

[13] L.K. Bagal, J.Y. Patil, K.N. Bagal, I.S. Mulla, S.S. Suryavanshi, Acetone vapour sensing characteristics of undoped and Zn, Ce doped SnO_2 thick film gas sensor, Mater. Res. Innov. 17 (2013) 98–105, https://doi.org/10.1179/1433075×12Y.0000000035.

[14] J. Li, M. Zheng, M. Yang, X. Zhang, X. Cheng, X. Zhou, S. Gao, Y. Xu, L. Huo, Three-in-one Ni doped porous SnO_2 nanorods sensor: controllable oxygen vacancies content, surface site activation and low power consumption for highly selective NO_2 monitoring, Sens. Actuators. B 382 (2023) 133550, https://doi.org/10.1016/j.snb.2023.133550.

[15] S.u.Rahman Zulfiqar, T. khan, R. Khan, G. Khan, S. Khattak, N. Rahman, S. Ali, T. Hua, Dielectric and ferromagnetic properties of (Ni, Co) co-doped SnO_2 nanoparticles, J Mater Sci: Mater Electron 32 (2021) 19859–19870, https://doi.org/10.1007/s10854-021-06510-4.

[16] J. Divya, A. Pramothkumar, S. Joshua Gnanamuthu, D.C. Bernice Victoria, P. C Jobe prabakar, Structural, optical, electrical and magnetic properties of Cu and Ni doped SnO_2 nanoparticles prepared via Co-precipitation approach, Phys. B Condens. Matter. 588 (2020) 412169, https://doi.org/10.1016/j.physb.2020.412169.

[17] W. Darenfad, N. Guermat, Kamel Mirouh, Thoughtful investigation of ZnO doped Mg and co-doped Mg/Mn, Mg/Mn/F thin films: a first study, J. Mol. Struct. 1286 (2023) 135574, https://doi.org/10.1016/j.molstruc.2023.135574.

[18] W. Darenfad, N. Guermat, N. Bouarissa, F.Z. Satour, A. Zegadi, K. Mirouh, Improvement in optoelectronics and photovoltaic properties of p-Co_3O_4/n-ZnO hetero-junction: effect of deposition time of sprayed Co_3O_4 thin films, J. Mater Sci: Mater Electron. 35 (2024) 162, https://doi.org/10.1007/s10854-023-11909-2.

[19] D. Toloman, A. Popa, M. Stefan, T. Danut Silipas, R. Crina Suciu, Enhanced photocatalytic activity of Co doped SnO_2 nanoparticles by controlling the oxygen vacancy states, Opt. Mater. 110 (2020) 110472, https://doi.org/10.1016/j.optmat.2020.110472.

[20] A.A. Dakhel, Study of structural, optical and magnetic properties of hydrogenated Ni and (Ga, Zn) co-doped SnO_2 nanocomposites, Mater. Chem. Phys. 252 (2020) 123163, https://doi.org/10.1016/j.matchemphys.2020.123163.

[21] Z. Belamri, W. Darenfad, N. Guermat, Impact of Annealing Temperature on Surface Reactivity of ZnO Nanostructured Thin Films Deposited on, Aluminum Substrate J. Nano Electron. Phys. 15 (2023) 02026, https://doi.org/10.21272/jnep.15(2).02026.

[22] N. Guermat, A. Bellel, S. Sahli, Y. Segui, P. Raynaud, Thin plasma-polymerized layers of hexamethyldisiloxane for humidity sensor development, Thin. Solid. Films 517 (2009) 4455–4460, https://doi.org/10.1016/j.tsf.2009.01.084.

[23] N. Guermat, A. Bellel, S. Sahli, Y. Segui, P. Raynaud, Plasma polymerization of hexamethyldisiloxane and tetraethoxysilane thin films for humidity sensing application Defect and Diffusion Forum 354 (2014) 41–47. doi:10.4028/www.scientific.net/DDF.354.41.

[24] M.I. Amer, S.H. Moustafa, M. El-Hagary, Enhanced band structure, optoelectronic and magnetic properties of spray pyrolysis Ni-doped SnO_2 nanostructured films, Mater. Chem. Phys. 248 (2020) 122892, https://doi.org/10.1016/j.matchemphys.2020.122892.

[25] M.H. Abdi, N.B. Ibrahim, Microstructure, electrical and magnetic properties of nickel doped tin oxide film prepared by a sol – gel method followed by a nitrogen annealing process, Physica B 581 (2020) 411758, https://doi.org/10.1016/j.physb.2019.411758.

[26] A.E. Shalan, M. Rasly, I. Osama, M.M. Rashad, I.A. Ibrahim, Photocurrent enhancement by Ni^{2+} and Zn^{2+} ion doped in SnO_2 nanoparticles in highly porous dye-sensitized solar cells, Ceram. Int. 40 (2014) 11619–11626, https://doi.org/10.1016/j.ceramint.2014.03.152.

[27] W. Daranfed, N. Guermat, K. Mirouh, Experimental study in the effect of precursors in Co_3O_4 thin films used as solar absorbers, Ann. Chim.-Sci. Mat. 44 (2020) 121–126, https://doi.org/10.18280/acsm.440207.

[28] L. Kumar Gaur, M. Chandra Mathpal, P. Kumar, S.P. Gairola, V. Agrahari, M.A. R. Martinez, F.F.H. Aragon, M.A.G. Soler, H.C. Swart, A. Agarwal, Observations of phonon an harmonicity and microstructure changes by the laser power dependent Raman spectra in Co doped SnO_2 nanoparticles, J. Alloys. Compd. 831 (2020) 154836, https://doi.org/10.1016/j.jallcom.2020.154836.

[29] R. Ramarajan, M. Kovendhan, K. Thangaraju, D. Paul Joseph, R. Ramesh Babu, V. Elumalai, Enhanced optical transparency and electrical conductivity of Ba and Sb co-doped SnO_2 thin films, J. Alloys. Compd. 823 (2020) 153709, https://doi.org/10.1016/j.jallcom.2020.153709.